



China Geology

Journal homepage: <http://chinageology.cgs.cn>
<https://www.sciencedirect.com/journal/china-geology>



Natural gas hydrates in the Qinghai-Tibet Plateau: Characteristics, formation, and evolution

You-hai Zhu, Shou-ji Pang*, Rui Xiao, Shuai Zhang, Zhen-quan Lu

Oil and Gas Resources Survey, China Geological Survey, Beijing 100083, China

ARTICLE INFO

Article history:

Received 1 March 2021
 Received in revised form 18 March 2021
 Accepted 21 March 2021
 Available online 23 March 2021

Keywords:

Natural gas hydrates (NGH)
 Permafrost
 Global climate change
 Qinghai-Tibet Plateau

ABSTRACT

The Qinghai-Tibet Plateau (also referred to as the Plateau) is the largest area bearing alpine permafrost region in the world and thus is endowed with great formation conditions and prospecting potential of natural gas hydrates (NGH). Up to now, one NGH accumulation, two inferred NGH accumulations, and a series of NGH-related anomalous indicators have been discovered in the Plateau, with NGH resources predicted to be up to 8.88×10^{12} m³. The NGH in the Qinghai-Tibet Plateau have complex gas components and are dominated by deep thermogenic gas. They occur in the Permian-Jurassic strata and are subject to thin permafrost and sensitive to environment. Furthermore, they are distinctly different from the NGH in the high-latitude permafrost in the arctic regions and are more different from marine NGH. The formation of the NGH in the Plateau obviously couples with the uplift and permafrost evolution of the Plateau in spatial-temporal terms. The permafrost and NGH in the Qilian Mountains and the main body of the Qinghai-Tibet Plateau possibly formed during 2.0–1.28 Ma BP and about 0.8 Ma BP, respectively. Under the context of global warming, the permafrost in the Qinghai-Tibet Plateau is continually degrading, which will lead to the changes in the stability of NGH. Therefore, The NGH of the Qinghai-Tibet Plateau can not be ignored in the study of the global climate change and ecological environment.

©2021 China Geology Editorial Office.

1. Introduction

NGH are ice-like solid substances formed from hydrocarbon gases dominated by methane and water under low-temperature and high-pressure conditions. They mainly occur in submarine sediments and terrestrial permafrost. They are a new type of potential energy source with great energy potential. It is predicted that the global resources of NGH are up to 2.1×10^{16} m³ (Kvenvolden KA, 1988; Milkov AV, 2004). Additionally, they have significant implications for the environment and ecology. Therefore, they have attracted high attention all over the world. The perennial permafrost in China covers an area of about 2.5×10^6 km², which makes China rank as the third largest country in terms of permafrost. They are mainly distributed in the Qinghai-Tibet Plateau and Da Hinggan Mountains areas. Among them, the Qinghai-

Tibet Plateau is the main body bearing permafrost with an area of about 1.5×10^6 km², and the permafrost is typical alpine perennial permafrost (Zhou YW et al., 2000). The Qinghai-Tibet Plateau boasts great formation conditions and prospecting potential of NGH (Xu XZ et al., 1999; Ku XB et al., 2007; Zhu YH et al., 2011). Furthermore, NGH samples have been obtained by drilling and a series of anomalous indicators have been discovered in the Plateau, proving that China is one of a few countries where both marine and terrestrial NGH are stored. However, the detailed characteristics of the NGH in the Qinghai-Tibet Plateau are yet to be systemically summarized under global vision. Moreover, the formation and evolution of the NGH in the Qinghai-Tibet Plateau are to be further studied under the context of global warming and permafrost degradation. This paper systemically summarizes the main characteristics of the NGH in the Qinghai-Tibet Plateau and discusses their formation and evolutionary history based on more than ten years' research achievements gained by survey teams of NGH in terrestrial permafrost affiliated to the China Geological Survey (CGS) as well as a large amount of literature.

First author: E-mail address: 1768210693@qq.com (You-hai Zhu).

* Corresponding author: E-mail address: psj0409@163.com (Shou-ji Pang).

doi:10.31035/cg2021025

2096-5192/© 2021 China Geology Editorial Office.

2. Basic characteristics of NGH in the Qinghai-Tibet Plateau and comparison with arctic permafrost regions

Three NGH accumulations and a series of NGH-related anomalous indicators have been discovered in the Qinghai-Tibet Plateau currently, including one NGH accumulation discovered in the Muli area in the South Qilian Basin, two inferred NGH accumulations found out in Kunlun Pass Basin and Wuli area in southern Qinghai Province, and a series of anomalous indicators revealed in the Qiangtang Basin and Halahu Depression of the South Qilian Basin (Fig. 1). NGH in the Plateau are all occurred under permafrost zone, mainly occur in consolidated Mesonic strata, and are mostly distributed in sandstone pores and shale fractures. They are dominated by thermogenic gases, are controlled by the fault and fissure structures, and are well trapped (Table 1).

2.1. Distribution characteristics of NGH

The Muli Depression in the South Qilian Basin was formed during Late Paleozoic–Mesozoic based on the Early Paleozoic tectonic evolution. It is the first NGH accumulation found in the middle-latitude alpine permafrost region in the world, where the NGH were firstly discovered in 2008 (Fig. 2). So far, the CGS and the China Shenhua Energy Co. Ltd. (Qinghai) have drilled 25 wells for NGH exploration and four wells for NGH production test in the depression, discovering NGH samples in 11 exploration wells and four production

wells and NGH anomalies in the remaining wells. It was discovered that the NGH in the depression are produced under the permafrost, with a burial depth of 133–396 m, and they mainly occur in the Middle Jurassic Jiangcang Formation (Zhu YH et al., 2010; Li B et al., 2017; Wang PK et al., 2019).

The Kunlun Pass Basin is a Pliocene–Middle Pleistocene fault basin with an area of about 50 km², where about 600 m thick Neogene–Quaternary sediments were deposited. The well KZ-3 was drilled in the basin in 2013, through which a series of evidence of NGH occurrence was inferred. For instance, large amounts of gases were observed releasing in multiple strata at a depth of more than 250 m, which contains methane of about 22%–32% and have the characteristics of intermittent release of NGH dissociation. Furthermore, the gas-release horizons show logging characterized by low density and increase in lateral resistivity and sonic velocity. Meanwhile, marks of authigenic minerals associated with NGH dissociation such as authigenic carbonate and pyrite were found. All these indicate that NGH may occur in the basin (Wu QB et al., 2015).

The Wuli area in Qinghai Province is located on the northwestern margin of the Qiangtang Basin. The wells TK-2 and TK-3 were successively drilled in this area in 2015–2016. As a result, strong bubbling and “sweating” phenomena (gas and water release after hydrate dissociation) were found in the core taken from Permian Nayixiong Formation at a depth of

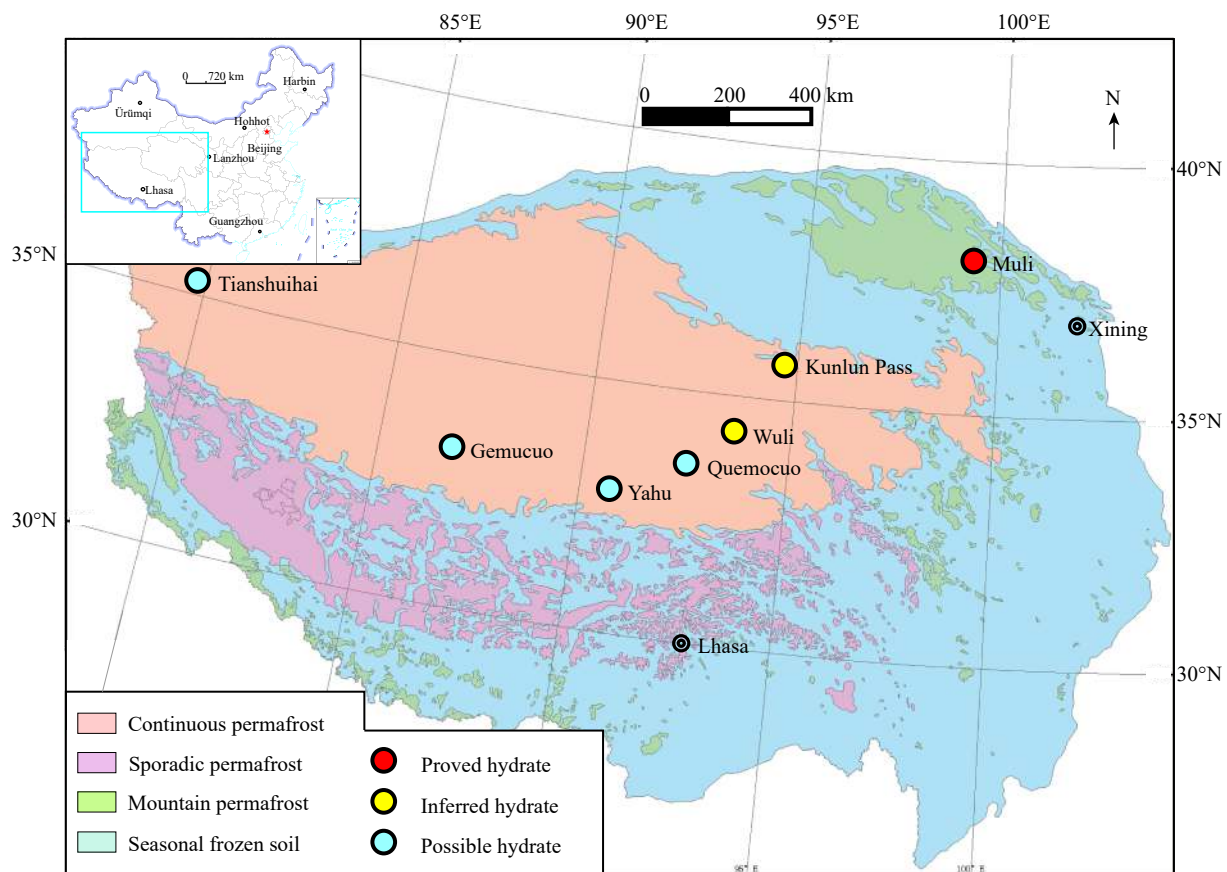


Fig. 1. Distribution of NGH in the Qinghai-Tibet Plateau.

Table 1. Summary of the properties of global NGH in permafrost.

Location	Main evidences	Distribution	Burial depth/m	Strata	Occurrence	Content of methane/%	Gas origin	Permafrost type	H_p /m	$T_g/^\circ\text{C}$	$G_p/^\circ\text{C}/\text{km}$	$G_g/^\circ\text{C}/\text{km}$	Reference
Qilian Mountains, China	Samples	Below permafrost zone	133–396	Top Jurassic	Thin-bedded, flaky, cloddy, and disseminated	66–94	Thermogenic	Alpine permafrost	110	-1.67	2.5	3.45	Zhu YH et al., 2010
Kunlun Pass, China	Logging and geochemistry	Below permafrost zone	257–439	Quaternary and Triassic		22–32	Thermogenic mixed with biogenic	Alpine permafrost	81.5–112	-2.9	2.4–3.6	2.5–4.9	Wu QB et al., 2015
Wuli, China	Logging and geochemistry	Below permafrost zone	52–241	Permian		0.01–40	Thermogenic, inorganic mantle-derived CO_2	Alpine permafrost	20			3.0	Liu H et al., 2019
Messoyakha, Russia	Geochemistry	Below permafrost zone	720–820	Upper Cretaceous		98.6	Thermogenic mixed with biogenic	Arctic permafrost	420–480	-18	1.0	1.4	Makogon YF et al., 2007
Alaska, USA	Samples	Below permafrost zone	200–870	Paleogene - Neogene	Disseminated, nodular, and veined	91–99	Thermogenic mixed with biogenic	Arctic permafrost	174–630	-10	1.5–4.5	1.6–4.2	Dai S, 2011
Mackenzie, Canada	Samples	Below or in permafrost zone	890–1110	Oligocene - Holocene	Disseminated, veined, elastic, and nodular	91.2–99.5	Thermogenic	Arctic permafrost	510–740	-15–-20	1.8	2.7	Majorowicz JA et al., 2001

Notes: H_p —thickness of permafrost; T_g —Annual average ground temperature; G_p —geothermal gradient within permafrost; G_g —Geothermal gradient beneath permafrost.

52–241 m. They were associated with the marks such as infrared low-temperature anomalies and combustion-supporting ignition. The logging curves show the marks such as a decrease in density and increase in sonic velocity and lateral resistivity. Meanwhile, gas leak structures, authigenic minerals, and salting out phenomenon were observed. All these serve as the significant marks of NGH occurrence. Besides, as shown in the gas logging results of well TK-3, there are rich CO_2 manifestations in multiple layers of the Nayixiong Formation, and the CO_2 content is up to 91.09% with an average of 31.03%, implying that there may be CO_2 hydrates in the area (Liu H et al., 2019).

A series of anomalous indicators associated with NGH have been discovered in the Qiangtang and South Qilian basins in the Qinghai-Tibet Plateau, indicating the possible occurrence of NGH. The main anomalous indicators are stated as following. (1) Thick hydrocarbon source rocks and distinct hydrocarbon gas manifestations were found in Quemucuo area of Qiangtang Basin. The gas logging of well QK-8 shows the maximal total hydrocarbon content of 5.425% and the maximum methane content of 3.596%. (2) Shallow high-pressure gases were found in wells QK-6 and QK-7 in Yahu area of the Qiangtang Basin, and mud volcanoes were found in its adjacent Tucuo area. (3) A large number of mud volcanoes were found in Gemucuo area of the Qiangtang Basin, some of which are still emitting gases and thus are modern mud volcanoes. (4) Large-scaled mud volcanoes and their associated modern cold seep and cold seep carbonate were found in the Tianshuihai Basin, Xinjiang Uygur Autonomous Region. Meanwhile, hydrocarbon gas anomalies were also discovered in the basin. (5) The seismic profiles of the Halahu area in the South Qilian Basin show distinct velocity reversion and seismic reflection blanking zones. In addition, some indications for gas hydrate have been discovered in Mehe Basin, Northeastern China permafrost (Zhao XM et al., 2018).

The NGH in northern hemisphere permafrost are primarily stored in the frozen ground in the Arctic, including the West Siberia Basin and northern areas in Russia, the North Slope of Alaska in the United States, the Mackenzie Delta and Arctic Archipelago in Canada, and Svalbard and other islands in Norway (Collett TS et al., 2011). Among them, the Messoyakha in West Siberia Basin, Mackenzie Delta, and the North Slope of Alaska are most famous and have been produced test at present (Fig. 3; Table 1).

2.2. Characteristics of gas sources of NGH

A vast majority of marine hydrates are a microbial gas hydrates, except for the thermogenic gas hydrates in a minority of regions such as Black Sea and Gulf of Mexico. On the contrary, NGH in permafrost are mostly thermogenic gas hydrates (Dai JX et al., 2017), so does in the Qinghai-Tibet Plateau. The NGH in the Muli area consist of relatively complex gas components. They contain large quantities of methane as well as heavy hydrocarbon components such as ethane and propane, and some NGH samples even contain a



Fig. 2. Photos of drilling site and NGH burning in the Muli area of South Qilian Basin.

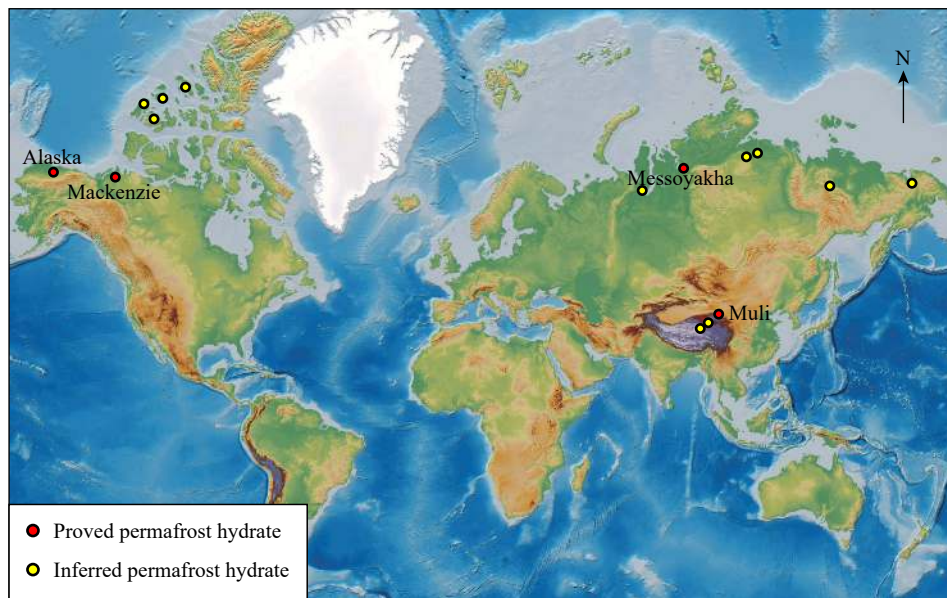


Fig. 3. Distribution of global NGH in permafrost.

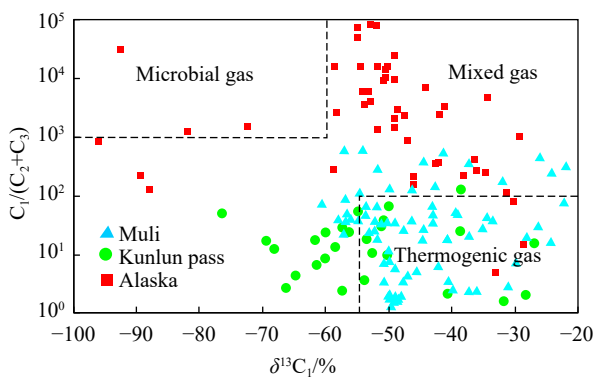


Fig. 4. Gas source types of global NGH in permafrost (the data of Kunlun Pass Basin from Wu QB et al., 2015; data of Alaska from Collett TS et al., 1990 and Lorenson TD et al., 2011).

certain quantity of CO_2 . Therefore, the NGH in the Muli area are rare (Zhu YH et al., 2010). The $\delta^{13}\text{C}_1$ values of methane in the NGH mainly range between -31.3% and -52.6% , and

thus the NGH mainly originate from thermogenic gas, which is associated gases of crude oil, and some of the NGH are mixed gases (Fig. 4). The NGH in the Muli area are formed from as deep thermogenic gases migrate to the shallow hydrate stability zones through faults and then are covered by the overlying permafrost.

The gas sources of NGH in the Kunlun Pass Basin are thermogenic gases and mixed gases. The analytical results of desorbed gases and mud gases of the cores taken from four wells in the basin indicate that the gases mainly consist of methane and trace of ethane and propane. Among the four wells, wells ZK1 and ZK2 are shallow and only the Quaternary Qiangtang Formation was revealed, and the gases have low content of methane and thus are *in-situ* microbial gas hydrates. Wells ZK3 and ZK4 are deep, and the gases have obviously higher content of methane and thus are mixed gases, indicating that they are blended with the thermogenic gases originating from underlying Triassic Bayan Har Group and deep strata (Xiao HP et al., 2016). The gases revealed by

the wells ZK1 and ZK2 have high content of CO₂ with $\delta^{13}\text{C}_{\text{CO}_2}$ values of -26.8‰ – -20‰ , indicating that the CO₂ is organic gas (Zhang JH et al., 2016).

The gas sources in the Wuli area are more complicated. As indicated by the analytical results of 65 samples of on-site desorbed gases and water-soluble gases, the gases in the area mainly consist of CO₂ and a small amount of CH₄. Among them, the content of CO₂ is as high as 69.66%–99.98%, with an average of 98% and the content of CH₄ is 0.01%–40% and is 16.3% on average for four samples with high content of CH₄. Meanwhile, the CH₄ has relatively heavier $\delta^{13}\text{C}_1$ values, which are up to -27.82‰ – -32.38‰ . Therefore, it can be inferred that the gases originate from thermogenic gas and are mainly coal-bed methane gases, not excluding the possibility that they are blended with some inorganic gas. Meanwhile, the $\delta^{13}\text{C}_{\text{CO}_2}$ values are also relatively heavier, which are -13.9‰ – -1.18‰ and are dominated by -4‰ – -6‰ . Therefore, the CO₂ should be inorganic gas (Gong JM et al., 2014) and most likely are mantle-derived CO₂.

The Mackenzie Delta in Canada features pretty complex gas sources. Lorenson TD et al. (1999) analyzed the gases of well Mallik 2L-38, including the gas components and carbon isotopes of CH₄ in the gases. According to their analytical results, the hydrocarbon gases revealed by the well are mixed gases dominated by thermogenic gas and show obvious regular changes with depth. In detail, at a depth of shallower than 350 m, the gases are microbial gases with high content of CH₄ and very light carbon isotopes of CH₄. At a depth of 350–785 m, the gases are mixed gases, with the content of thermogenic gases being higher and the carbon isotopes of CH₄ growing heavier with an increase in depth. At a depth of 785–1165 m (bottomhole), the gases are thermogenic gases. This indicates that NGH at this depth mainly originate from deep thermogenic gases, which migrate to the hydrate stability zones through faults and so on to form hydrate. The NGH in the North Slope of Alaska also consist of methane primarily, ethane and propane secondarily, and a very small amount of other gases. Their genetic types are similar to those of the NGH in Mackenzie Delta and they are also mixed gases dominated by thermogenic gases. Lorenson TD et al. (2011) obtained the samples and test results from the Mount Elbert Gas Hydrate Stratigraphic Test Well and the details are as follows. At a depth of 0–200 m, the gasses are typical microbial gases since the $\delta^{13}\text{C}_1$ values of CH₄ are -80‰ – -86‰ . The strata at a depth of 200–600 m serve as a distinct transition zone. The gasses at this depth are mixed gases since the $\delta^{13}\text{C}_1$ values of CH₄ are -45‰ – -80‰ . At a depth of more than 600 m, the carbon isotopes of CH₄ are heavier and very stable, with $\delta^{13}\text{C}_1$ values of -42‰ – -48‰ . Therefore, the NGH are typical thermogenic gas and are possibly associated with bio-degradation.

Little data are reported in publications on gas sources of the NGH in Messoyakha, Russia currently. However, under the hydrate layers in the area lies the Messoyakha gas field, of which the content of CH₄, ethane, propane, CO₂, and nitrogen is 98.6%, 0.1%, 0.1%, 0.5%, and 0.7%, respectively

(Makogon YF et al., 2007). Therefore, the hydrates in this area should be thermogenic gas.

2.3. Characteristics of NGH reservoirs

The NGH reservoirs in the Muli area are diagenetic rocks in the Middle Jurassic Jiangeang Formation (Fig. 5). They are comprised of oil shale, mudstone, siltstone, and fine- and medium-grained sandstone. There are two types of NGH in terms of occurrence patterns, namely fracture-filling and pore-filling hydrates. Among them, the fracture-filling hydrates are mostly white and milky and thin-bedded, flaky, and cloddy in shape. They occur on the fracture surface of siltstone, mudstone, and oil shale and are visible to naked eyes, and a single layer of them is merely a few millimeters thick. The pore-filling hydrates occur in the pores of fine-grained sandstone and siltstone in a disseminated shape, and they are invisible to naked eyes.

There are also two types of NGH reservoirs in the Kunlun Pass. One type is large numbers of fissures and tectonic fractured zones. They formed from metamorphic flysch, sand slate, and black shale in the lower Triassic Bayan Har Group due to tectonic activities. The other type is the fluvatile-lacustrine clastic sediments of the Neogene-Quaternary Qiangtang Formation. They have not been consolidated into rocks yet, with porosity of up to more than 20% (Wu QB et al., 2015). The hydrates in Wuli area, Qinghai Province mainly occurred in Upper Permian Nayixiong Formation. The reservoirs mainly consist of gray and dark gray argillaceous siltstone, siltstone, gray fine-grained sandstone, and argillaceous fine-grained sandstone, interbedded with a few coal seams. The measured porosity of the cores is 2.25%–16.61%, with an average of 5.03%, and the permeability is 0.479–0.132 mD, with an average of 0.261 mD. Therefore, the reservoirs in the area are generally dense, but the cores are broken, which is favorable for occurrence of fracture-filling hydrates.

The hydrates in the Mackenzie Delta, Canada mainly occur in the clastic sediments of Paleogene Kugmallit Sequence and Neogene Mackenzie Bay and Iperk sequences, which are unconsolidated-weakly cemented. Most of the hydrates are stored below permafrost and only a few of them are occurred within permafrost. Among them, five hydrate layers were discovered at a depth of 897.25–1109.8 m in the well Malik 2L-38, with accumulative thick of up to 113 m. The hydrates occur in the coarse sands primarily and in the silty sediments partially. Meanwhile, some thin hydrates in veined, clastic, or nodular shapes are occasionally visible. All these indicate that the hydrates are under strong control of the lithology. The logging data indicate that there is a thin free gas layer below the bottom of the lowest hydrate layer. Meanwhile, there is a positive correlation between hydrate saturation and the content of sand in the sediments. That is, the higher the content of sand, the higher the hydrate saturation (Dallimore SR and Collett TS, 1999).

The hydrate reservoirs in the North Slope of Alaska are

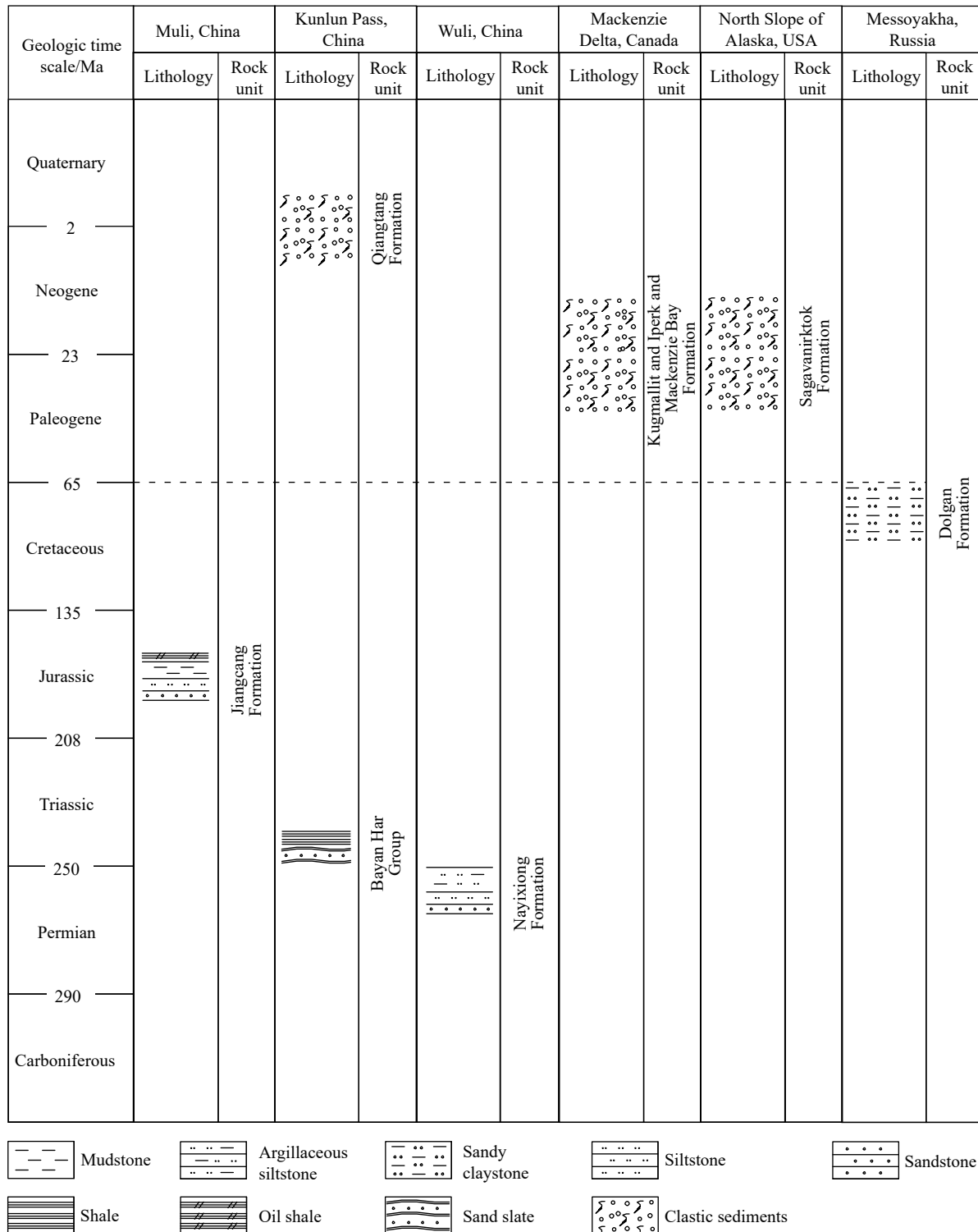


Fig. 5. Comparison among global NGH reservoirs in permafrost regions.

similar to those in the Mackenzie Delta. All of them are stored in Paleogene-Neogene Sagavanirktok Formation and are coastal-delta sands. Among them, the sand layer C in the Mount Elbert Gas Hydrate Stratigraphic Test Well is composed of hydrate-bearing sand with a thickness of 16 m (burial depth: 650–666 m), and the overlying sand layer D is composed of hydrate-bearing sand with a thickness of 14 m (burial depth: 614–628 m). Meanwhile, there is also a positive

correlation between the hydrate saturation and the grain size of sediments (Kneafsey TJ et al., 2011).

The hydrates in Messoyakha, Russia are located in the West Siberia Basin. The basin is a large anticline with a size of 12.5 km×19 km, covering an area of about 237 km². The hydrate layers are occurred in the core of the anticline, with a burial depth of 750–836 m and a thickness of about 84 m. Under them lies the Messoyakha gas field, and thus the

hydrate layers play a role in trapping natural gas reservoirs. The hydrate reservoirs are comprised of sandy claystone in the Upper Cretaceous Dolgan Formation, with a temperature of 8–12°C and pressure of 7.8 MPa. Meanwhile, the porosity of the reservoirs is 16%–38%, with an average of 25%, and the permeability of the reservoirs is 10–1040 mD, with an average of 203 mD (Makogon YF et al., 2007).

2.4. Characteristics of NGH cap rock (permafrost)

The gas sources of hydrates in permafrost mostly originate from deep thermogenic gases. The seal of permafrost is necessary to form NGH when the deep thermogenic gases migrate upwards the gas hydrate stability zone. The reason is that the permafrost can effectively prevent the free gases escape due to its extremely low permeability, and thus serves as an important trap for the formation of NGH.

The Plateau is the largest permafrost region in China. It covers an area of 1.50×10^6 km², which amounts for 69% of the total permafrost area in China. Furthermore, the permafrost in the Plateau is typical alpine permafrost and has the characteristics of high elevation, high annual average ground temperature, thin permafrost zone, and poor stability. The Qiangtang Basin is the area where permafrost is the most developed in the Plateau. The permafrost in the basin is continuously distributed. Furthermore, from the basin to its surrounding areas, the annual average ground temperature gradually increases, and thus the permafrost gradually grows thinner. As a result, the continuous permafrost is gradually transformed into island-shaped permafrost. The drilling results indicate that the permafrost in the Kunlun Pass Basin is 81.5–112 m thick while those in the Wuli area are only about 60 m since the Wuli area falls in a melting area.

The Qilian Mountains permafrost region is located on the northern margin of the Qinghai-Tibet Plateau, with an area of about 0.1×10^6 km². It is an alpine permafrost region but is classified as a mountain permafrost region according to the division method proposed by Zhou YW et al. (2000). In this region, the annual average ground temperature is –1.5–2.4°C, and the permafrost thickness is generally 50–139 m. The Muli area is the central of the Qilian Mountains permafrost region, where perennial permafrost is continuously distributed except for local areas. The annual average ground temperature in the area is about –2.4°C. Meanwhile, according to the measurement in the ground temperature observation borehole DK-12 in the Muli area, the measured permafrost thickness is 110 m and the underground ice is usually visible.

In contrast to the Qinghai-Tibet Plateau, the hydrate accumulations in Messoyakha, Russia; Mackenzie, Canada; and the North Slope of Alaska, the United States are all located in the high-latitude areas. They are typical Arctic permafrost, with the characteristics of low elevation altitude, low annual average ground temperature, thick permafrost zone, and stable distribution. The permafrost thickness in these hydrate deposits is generally 400–500 m thick.

According to drilling results, the permafrost zone thickness in the Mackenzie Delta, the North Slope of Alaska, and Messoyakha is 640 m, about 600 m and 420–480 m, respectively, which are far greater than that of the Plateau.

2.5. Resource potential of NGH

In the early days, the potential hydrate resources were estimated as follows. First, delineate the area of potential NGH distribution regions according to the conditions such as temperature, pressure, and gas sources. Then, calculate the thickness of hydrate stability zones. Finally, estimate the potential hydrate resources by assuming some parameters. The NGH resources in the Plateau estimated in the early days differ greatly. They were estimated to be 0.12×10^{12} – 240×10^{12} m³ by Chen DF et al. (2005) based on hydrate stability zones, 45.3×10^{12} – 298×10^{12} m³ by Ku XB et al. (2007), and about 35×10^{12} m³ by Zhu YH et al. (2011) employing the volumetric method and the Monte Carlo method. With an increase in knowledge about NGH in recent years, the methods and parameters used to estimate NGH resources have been continually improved, and the accuracy of the estimated results have also been improved. Meanwhile, the estimated resources have gradually become smaller. For example, the resources were estimated to be 2.20×10^{12} m³ by Wang X et al. (2018). Recently, the authors calculated NGH resources in the Plateau according to the following procedures. First, the Muli area was selected as a reference due to its high exploration level. Then, the volumetric method was adopted to evaluate the NGH resources in the Muli area. After that, the resources in the South Qinlian Basin and Qiangtang Basin were calculated by analogical and genetic methods. Finally, the NGH resources in the Plateau was calculated and it is about 8.88×10^{12} m³, showing enormous resource potential (Table 2).

In contrast to the Plateau, the NGH resources in the North Slope of Alaska in the United States, Mackenzie (including the adjacent Beaufort Sea) in Canada, and Messoyakha in Russia are 0.71×10^{12} – 4.47×10^{12} m³ (median: 2.42×10^{12} m³), 2.4×10^{12} – 80.7×10^{12} m³, and 0.41×10^{12} – 4.47×10^{12} m³, respectively (Table 2). Ruppel C (2015) estimated the resources in the permafrost of the entire Arctic to be about

Table 2. Resources estimates of natural gas hydrates in permafrost.

Region	Resources / $\times 10^{12}$ m ³	References
Qinghai-Tibet Plateau	0.12–240	Chen DF et al., 2005
Qinghai-Tibet Plateau	45.3–298	Ku XB et al., 2007
Qinghai-Tibet Plateau	35	Zhu YH et al., 2011
Qinghai-Tibet Plateau	2.20	Wang X et al., 2018
Qinghai-Tibet Plateau	8.88	This study
Messoyakha, Russia	0.41–4.47	Makogon YF et al., 2007
Alaska, USA	2.42	Collett TS et al., 2011
Beaufort-Mackenzie, Canada	2.4–80.7	Majorowicz JA et al., 2001
Arctic Permafrost	40	Ruppel C., 2015

$40 \times 10^{12} \text{ m}^3$, which is similar to that of the Plateau.

3. Formation process of NGH

NGH form in a low-temperature and high-pressure environment. Permafrost provides a relatively low-temperature environment for the formation of NGH, and it provides cap rock for the deep gas sources that migrate upwards to avoid gas escape. Therefore, the key to the formation of NGH is that the gas sources, permafrost, and temperature/pressure conditions are well matched. Meanwhile, the formation of the NGH closely couples with the uplift and permafrost evolution of the Plateau in spatial-temporal terms.

3.1. Uplift process of the Qinghai-Tibet Plateau

The uplift of the Plateau was a result of the collisions between the Indian and Eurasian plates. The continent-continent collisions between the two plates occurred in about 65–60 Ma BP. As the Indian Plate gradually drifted and extruded northwards (it is estimated that the Indian Plate drifted about 2500–3000 km northwards according to magnetic anomaly belts), the Tethys Ocean disappeared and a plateau rose and finally formed the Plateau of today. There are different opinions on the uplift eras and process of the Plateau. Among them, the one most widely accepted is the multi-stage, uneven, and varying-speed uplift pattern consisting of “three stages of uplift and two-time deplaning” proposed by Shi YF et al. (1999). In detail, it states that the Plateau rose in 45–38 Ma BP, 25–17 Ma BP, and 3.6 Ma BP - now and that it was razed to ground twice during three uplifting. The Plateau only rose to a small extent in the first two stages on the whole, and the average elevation of the Plateau was not greater than 2000 m. In contrast, the sharpest uplift occurred at the third stage after 3.6 Ma BP. Zhong DL and Ding L (1996) argued that there is the fourth uplift, i.e. the uplift during 13–8 Ma BP, according to numerous fission-track ages of apatite in eastern Himalaya. Meanwhile, Ge XH et al. (2014) simplified the three-stage uplift into two stages, i.e. 23–17 Ma BP and 3.6–0.8 Ma BP, based on the evolutionary characteristics of sedimentary structures in the

Qaidam Basin. Despite different opinions on the number of uplift stages, it is agreed that the quick uplift occurring after 3.6 Ma BP is the most important one in the formation process of the Plateau.

3.2. Formation process of permafrost in the Qinghai-Tibet Plateau

The permafrost in the Plateau formed mainly due to the decrease in the ground temperature caused by the uplift of the Plateau. However, it is difficult to accurately determine the exact formation era. The quick uplift of the Plateau was caused by the “Qinghai-Tibet Movement” starting in 3.6 Ma BP, which is represented by strong uplift, disruption of the main planation surface, and the formation of large fault basins. Its elevation rose to about 2000 m in 2.5 Ma BP, reaching the “dynamic critical height” affecting the atmosphere. As a result, it is difficult for monsoon to climb over the Plateau, and thus the modern monsoon pattern in which the wind system circulates around the Plateau was formed. The later period of 1.1–0.6 Ma BP during which Kunlun-Yellow River tectonic movement happened is another important uplift state of the Plateau. As a result, the average elevation of the Plateau reached around 3000–3500 m during 0.8–0.5 Ma BP, with the elevation of the mountainous area even reaching up to more than 4000 m (Shi YF et al., 1999; Zheng D et al., 2002; Li JJ, 2013).

The Middle Pleistocene Transition (MPT) and global cooling exactly happened about 0.8 Ma BP. The former is one of the most important events in Quaternary climate change, which the main climatic oscillations from 41 ka transform to 100 ka in the Middle Pleistocene (Lu J and Chen MH., 2006). In around 0.8 Ma BP, the quick uplift of the Plateau, the transition of the climatic oscillation cycle, and the global cooling were coupled with each other. As a result, the Plateau entered the cryosphere, a large scale of glaciers developed, and accordingly a large area of perennial permafrost began to form. After that, the Plateau continued rising and the average elevation of the Plateau surface gradually rose to more than 4000 m. Despite a short change of climate between glacial and interglacial periods, the main part of the Plateau has

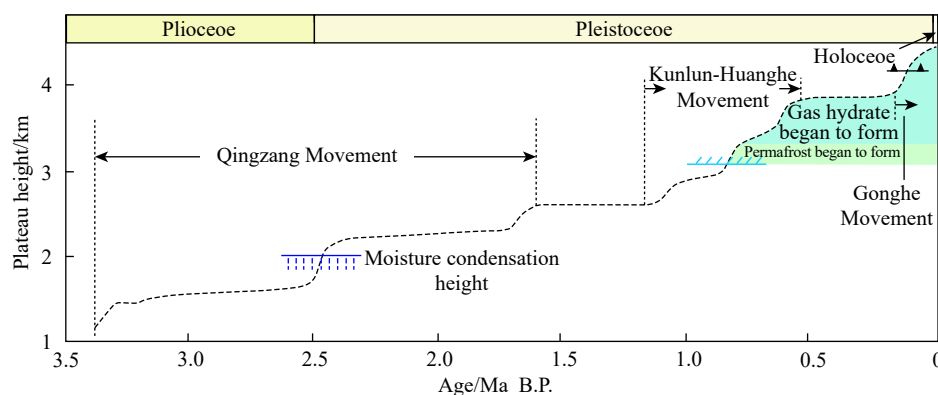


Fig. 6. Illustration of the uplift of the Qinghai-Tibet Plateau and the formation of the permafrost and NGH in the Qinghai-Tibet Plateau (the data on uplift and permafrost formation modified from Shi YF et al., 1999).

always remained frozen (Fig. 6).

Qiao YC et al. (2010) calculated the initial formation time of the permafrost in the Plateau at different uplift rates by simulation with the finite element method. According to the simulation results, the formation era of the permafrost and the current permafrost thickness in the Plateau should be about 0.39 Ma and 124.68 m, respectively assuming that the Plateau rose from 1000 m to 5000 m at an uplift rate of 2 mm/a in 2 Ma, while they should be about 0.98 Ma and 129.95 m, respectively assuming that the Plateau rose from 1000 m to 5000 m at an uplift rate of 0.8 mm/a in 5 Ma. The second results are roughly consistent with the above-mentioned formation eras, i.e., about 0.8 Ma BP.

There is a lack of consensus on the formation era of the glaciers and permafrost in the Qilian Mountains. Pan BT et al. (1995) and Li QL et al. (2003) thought that they formed in the early stage of the Early Pleistocene and the details are as follows. During 2.0–1.28 Ma BP, the Qilian Mountains quickly rose for the first time, leading to decrease in atmospheric temperature and the first occurrence of massive glacial activities. As a result, permafrost started to form in the area. During 1.05–0.36 Ma BP especially around 0.8 Ma BP, the Qilian Mountains experienced the second quick uplift. Consequently, the main body of the Qinghai-Tibet Plateau entered the cryosphere, leading to the largest scale of glaciers in the Qilian Mountains. Li JJ et al. (2013) considered that the glaciers and permafrost in the Qilian Mountains formed in the Middle Pleistocene and the main reason is the Kunlun-Yellow River tectonic movement occurring around 0.8 Ma BP, which is roughly the same as the formation time of the main body of the Qinghai-Tibet Plateau. They even restricted the formation era to 0.47–0.45 Ma BP, which is consistent with oxygen isotope stage 12 (MIS12; Zhou SZ and Li JJ, 2003). Recently, Qi BS et al. (2014) found original sand wedge groups in Middle Pleistocene alluvial-diluvial sand gravel layers on the north bank of the Qinghai Lake. The ages of two of the sand wedges determined by ESR dating are 0.773 ± 0.070 Ma BP and 0.774 ± 0.070 Ma BP, indicating that the Qilian Mountains had largely entered the freeze period and glaciers had spread to the Qinghai Lake about 0.77 Ma BP. Based on this as well as the high latitude and relatively early uplift of the Qilian Mountains, the authors agree with the first opinion, i.e., the permafrost in the Qilian Mountains possibly formed in 2.0–1.28 Ma BP, which is earlier than the formation time of the main body of the Qinghai-Tibet Plateau.

Different from the Qinghai-Tibet Plateau, the permafrost in arctic regions formed earlier. The formation era should be 3.6–2.6 Ma BP, which is basically in the same as that of the Arctic ice sheet. Glaciers first appeared on the Arctic land in the late Middle Miocene. Then they gradually spread over the land in stages until formed the giant Arctic ice sheet during 2.8–2.6 Ma BP. Most researchers consider that the formation mechanism of the giant Arctic ice sheet is related to the uplift of the Qinghai-Tibet Plateau or the closure of the Panama Seaway (An ZS et al., 1998).

3.3. Formation process of NGH in the Qinghai-Tibet Plateau

Due to the lack of direct methods, the formation ages of NGH can only be indirectly inferred from the factors such as the formation and migration of hydrocarbon gases and coverage of permafrost. For example, Zhou Q et al. (2011) held that the primary hydrocarbon-generating periods of major oil basins in the Plateau are the Late Jurassic–Early Cretaceous, and that NGH finally formed after the quickly uplift of the Plateau, the drastic drop in temperature, and permafrost formation since 3.4 Ma BP. Lu et al. (2018, 2020) also indicates that NGH in the Muli area formed over three stages, namely the generation and enrichment of hydrocarbon during the Middle Jurassic, the uplift and erosion of strata and gas migration during Early Cretaceous–Pliocene, and frost action and the formation of hydrate reservoirs in the early stage of the Middle Pleistocene.

NGH should form later than permafrost. In other words, permafrost occurs earlier than hydrates. As stated above, the permafrost in the Qilian Mountains possibly formed during 2.0–1.28 Ma BP, which might be the initial formation time of the hydrates in the permafrost in the Qilian Mountains.

In the Kunlun Pass Basin, the hydrocarbon source rocks in the Triassic and deep strata were highly matured and produced massive hydrocarbon gases during the Cenozoic. About 0.8 Ma BP, the basin entered the cryosphere and permafrost gradually formed. Owing to some faults and their associated secondary fissures forming during the neo-tectonic movement since 0.6 Ma BP, the residual hydrocarbon gases in the deep strata migrate upwards and gradually form NGH under the coverage of the permafrost (Xiao HP et al., 2016).

The formation progress of the NGH in the North Slope of Alaska in the United States and Mackenzie in Canada is a little different from that in the Plateau. NGH in these areas possibly formed earlier than permafrost, since these areas fall into the same hydrate-oil system with the Beaufort Sea. For instance, Dai S et al. (2011) simulated the depth-temporal evolution of hydrates and permafrost in Mount Elbert area in Alaska. The simulation results indicate that large-scale continuous permafrost began to form about 0.5 Ma BP (ground temperature below -5°C), while NGH began to form about 1.8 Ma BP in the area, showing a difference of about 1.3 Ma. The current hydrates in Mackenzie, Canada possibly formed a little later. The permafrost in the Mackenzie forming during the Illinoian Glacial Stage (115 ka BP) completely melted during the Sangamonian Interglacial Stage. As a result, all of the hydrates completely decomposed even if some hydrates formed. As of the Wisconsin Glacial Stage (starting about 85 ka BP), the permafrost formed again and kept thickening, and accordingly, NGH began to form. That is, the current hydrates in Mackenzie should have formed about 85 ka BP (Majorowicz JA et al., 2000).

4. Evolutionary process of NGH

NGH form and maintain stable only in a low-temperature and high-pressure environment. Otherwise, they will

decompose or form again. After the Plateau entered the cryosphere 0.8 Ma BP, the permafrost and NGH changed with global climate change, especially the transition between the glacial and interglacial periods, which in turn impacted the global climate change.

4.1. NGH in the Last Glacial Maximum

The Last Glacial Maximum (LGM, 27–10 ka BP) is the coldest period in the Plateau since the late stage of the Late Pleistocene, during which perennial permafrost was the most developed. As calculated based on various relict permafrost and models, the permafrost in the Plateau massively spread towards its surrounding areas during the LGM. As a result, it covered most of the Qaidam Basin, the drainage basin of the Qinghai Lake, and the Gonghe Basin in the north, the upstream valley of the Yarlung Zangbo River in the south, and a large region in the east. It covered an area of about 2.71×10^6 km², which is about 40% larger than its current area. Compare to the current Qinghai-Tibet Plateau, the bottom boundary of the perennial permafrost in the Plateau was 1200–1400 m lower in general and 1700 m lower in the northeastern part during the LGM, and the average atmospheric temperature throughout the Plateau was 7–9°C lower (Shi YF et al., 1997; Jin HJ et al., 2019).

The NGH stability zones and their thickness are mainly controlled by the factors such as temperature, pressure, gas components, and pore water's salinity. Assuming that the gas components, pore water's salinity, and the geothermal gradient remain constant, the critical parameters affecting the NGH stability zones can be simplified into annual average ground temperature and permafrost thickness. According to more than six years of observation data from the NGH field observation station in the Muli area, the parameters related to the NGH stability zones include are as follows. The annual average atmospheric temperature is -3.6°C , the annual average ground temperature is -1.67°C , the permafrost thickness is 110 m, the geothermal gradient within permafrost is $1.51^\circ\text{C}/100$ m, the geothermal gradient under permafrost is $3.9^\circ\text{C}/100$ m, and the density of rock is $2.5 \text{ g}/\text{cm}^3$. If the average atmospheric temperature in the Plateau during the LGM was about 7–9°C lower than it is now (the median: 8°C), the annual average atmospheric temperature and the annual average ground temperature in the Muli area were -11.6°C and -6.39°C , respectively during the LGM (Table 3).

The permafrost thickness during the geologic history can

only be indirectly estimated using some parameters since they are difficult to measure. Li SX and Cheng GD (1996), Luo DL et al. (2012), and Liu GY et al. (2016) have proposed different formulas or methods for calculating the permafrost thickness. However, some parameters they used are also difficult to acquire. Assuming the geothermal gradients within and under permafrost since the quaternary were respectively the same as those now, it can be inferred that the permafrost thickness in the Muli area during the LGM was up to 636 m (Table 3).

Based on some parameters and relevant assumptions, the NGH stability zone and its thickness in the Muli area during various geological periods can be determined by simulation and calculation using the program CSMHYD developed by Sloan. The parameters include the above-mentioned annual average ground temperature and permafrost thickness; measured the geothermal gradients within and under permafrost, and measured gas components of NGH in the Muli area (i.e., CH₄: 65.05%; C₂H₆: 8.19%; C₃H₈: 12.62%; iC₄H₁₀: 1.35%; nC₄H₁₀: 3.17%; iC₅H₁₂: 0.38%; nC₅H₁₂: 0.51%; C₆₊: 2.91%; and CO₂: 5.86%; Lu ZQ et al., 2011). Meanwhile, it is assumed that the pore water is fresh water. According to the calculation results, the top and bottom boundaries of the NGH stability zone during the LGM were 8 m and 1355 m deep, respectively. Therefore, the thickness of the NGH stability zone was 1347 m, which is about twice as thick as the thickness of the current NGH stability zone. Therefore, if there were enough gas sources to form NGH during the LGM, the total NGH resources in the Qinghai-Tibet Plateau would have been up to 16.54×10^{12} m³ (Table 3; Fig. 7).

4.2. NGH in Holocene Megathermal Period

After the LGM, the perennial permafrost in the Plateau tended to degrade in general with the fluctuations and warming of the climate. Especially during the Holocene Megathermal Period (HMP, 8.5–3 ka BP), the Plateau suffered the most intensive, quickest, and widest permafrost degradation. As a result, the permafrost region substantially shrank and the bottom boundary of the permafrost was 300–500 m higher than it is now. Meanwhile, the perennial permafrost was distributed in the shape of islands. In mountain such as the Qilian Mountains, the permafrost only remained on the top or upper-middle part of some high mountains. During the HMP, the permafrost area in the

Table 3. Summary of the NGH evolution in the Qinghai-Tibet Plateau.

Era	Area of permafrost region/ 10^6 km ²	Annual average atmospheric temperature/ $^\circ\text{C}$	Annual average ground temperature/ $^\circ\text{C}^*$	Permafrost thickness/m*	Thickness of NGH stability zone/m	NGH resources/ 10^{12} m ³
LGM (26–10 ka BP)	2.71	-11.6	-9.67	636	1280	18.10
HMP (8.5–3 ka BP)	1.02	0.4–1.4	2.83	0	213	3.01
Present (2018 AD)	1.50	-3.6	-1.67	110	628	8.88
2099 AD	0.76–1.25	-0.69	2.33	0	253	3.58

Note: * data in these columns are based on measured data of the Muli area in the Qilian Mountains; other data are calculated according to formulas or assumed based on inferences in the context.

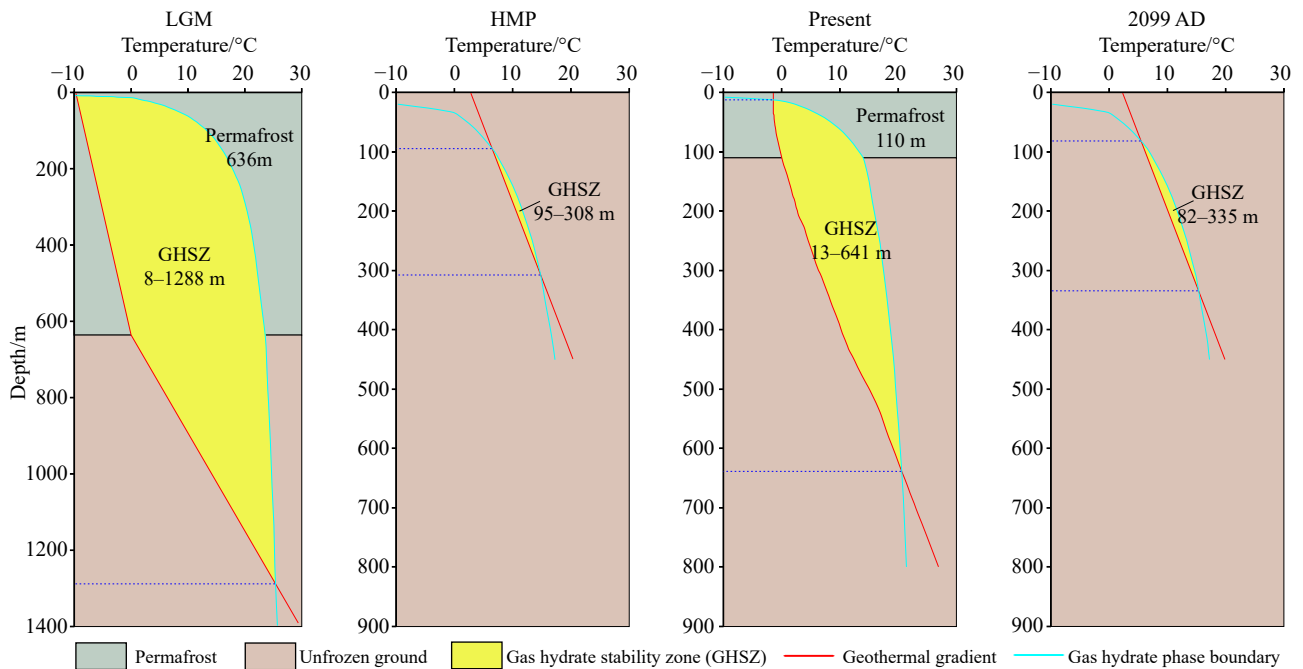


Fig. 7. Change of NGH stability zone in the Muli area during the LGM, the HMP, the present and 2099.

Plateau possibly reduced to $10.2 \times 10^3 \text{ km}^2$, which is about 73% of the current area. Thus the HMP is the period with the smallest area of the perennial permafrost in the Plateau. The annual average atmospheric temperature during the HMP was 4–5°C higher than it is now (Jiao SH et al., 2015; Jin HJ et al., 2019).

During the HMP, the ground temperature in the Muli area was up to 2.83°C, leading to the disappearance of perennial permafrost in the area. However, the hydrate stability zone still existed during this period due to the complex gas components and corresponding not very strict temperature and pressure conditions for the formation of hydrates in the area. According to the above-mentioned methods, the thickness of the NGH stability zone in the Muli area was merely 213 m and the NGH resources in the Plateau were about $3.01 \times 10^{12} \text{ m}^3$ during the HMP. Therefore, more than four-fifth of the NGH in the Plateau ($15.09 \times 10^{12} \text{ m}^3$) were decomposed from the LGM to the HMP.

4.3. NGH prediction under the background of global warming

The permafrost in the Plateau has the characteristics of wide distribution, thin thickness, high ground temperature, and poor stability, and thus is more sensitive to global climate change than that in arctic regions. Under the background of global warming, the Plateau suffered more significantly warming. For example, over the past 50 years, the rate of increase in temperature in the Plateau is twice as high as the global average rate of increase in temperature (Yao TD, 2019). During 1961–2017, the atmospheric temperature continuously increased at a rate of 0.045°C/a in the Qilian Mountains, which is clearly higher than the national average rate in the corresponding period (Dai S et al., 2019). As a result, the permafrost degraded to different extents, which is

represented by the increase in ground temperature, reduced in permafrost area, decrease in permafrost thickness or even disappearance, and expanse of melted region. For example, as for the perennial permafrost in the Plateau, the annual average ground temperature increased by about 0.1–0.5°C, the bottom boundary rose by 40–80 m, and the area reduced by about $100 \times 10^3 \text{ km}^2$ since the 1970s (Cheng GD et al., 2019). The simulation results show that the permafrost area in the Qilian Mountains also gradually reduced by $97.5 \times 10^3 \text{ km}^2$, $93.5 \times 10^3 \text{ km}^2$, $88.5 \times 10^3 \text{ km}^2$ and $76.6 \times 10^3 \text{ km}^2$ in the 1970s, 1980s, 1990s and 2000s, respectively (Zhang WJ et al., 2014).

The Qinghai-Tibet Plateau will further warm in the future. According to the 4th report issued by the Intergovernmental Panel on Climate Change (IPCC) in 2007, the global average atmospheric temperature will increase by 1.8–4.0°C as of 2099. Based on the predicted data, Jiao SH et al. (2016) simulated and calculated the permafrost degradation in the Plateau, and the results are as follows. In the case that the temperature rises by 1.8°C in 2099, the permafrost area in the Plateau will be $1.25 \times 10^6 \text{ km}^2$ in 2099, which is about 83.4% of the current area. In the case that the temperature rises by 4°C, the permafrost area in the Plateau will be $1.10 \times 10^6 \text{ km}^2$, which is about 73% of the current area. Assuming that the rate of increase in the temperature in the Plateau is higher than that in the whole globe, i.e. in the case that the temperature rises by 6°C, the permafrost area in the Plateau will be only $0.76 \times 10^6 \text{ km}^2$, which is about a half of the current area. The simulation results obtained by Li X and Cheng GD (1999) are similar to the above results. In detail, if the average atmospheric temperature in the Plateau increases by 1.10°C as of 2099, the permafrost region in the Plateau will reduce by 19%. If the average atmospheric temperature in the Plateau increases by 2.91°C as of 2099, the permafrost region in the

Plateau will reduce by 58.18% and the perennial permafrost will only exist in the northwestern part of the Plateau.

According to the above-mentioned methods, all of the permafrost will be melting but the NGH stability zone will still exist in the Muli area in 2099 if the average atmospheric temperature rises by 4.0°C in 2099. The thickness of the NGH stability zone will be merely 253 m, which is roughly similar to that during the HMP. Meanwhile, the NGH resources in the Plateau will be $3.58 \times 10^{12} \text{ m}^3$, which is basically similar to that during the HMP.

Assuming that the temperature continually rises in the same way and the ground temperature rises to 4.00°C, the NGH stability zone in the Muli area will completely disappear and almost all of the NGH will decompose.

5. Discussion

5.1. NGH comparison among permafrost regions worldwide

The NGH in the Plateau are different from those in the Arctic permafrost regions and are even more different from marine hydrates in terms of the gas source, reservoirs, permafrost conditions, formation mechanism, and formation age (Table 1). In terms of the gas source, hydrates in the Plateau mostly originate from deep thermogenic gases, which have high content of CO₂ in general. Most especially in the Wuli area, high-content CO₂ is extremely rare in the world and possibly is mantle-derived inorganic CO₂. The hydrates in Arctic permafrost regions also originate from deep thermogenic gases mostly, but they are mixed with shallow microbial gases more or less. In contrast, most of the marine hydrates come from shallow microbial gases (Dai JX et al., 2017).

In terms of reservoirs, the hydrates discovered in the Plateau all occur in consolidated Permian-Jurassic strata, which are mostly low-porosity and low-permeability strata. Most of the hydrates occur in rock fractures in the way of fissure filling, and only part of those in the Kunlun Pass Basin possibly occur in the Quaternary unconsolidated loose sediments. Similar to those in the Plateau, the reservoirs in Messoyakha, Russia are also consolidated ancient strata. The hydrates in the North Slope of Alaska, USA, and Mackenzie Delta, Canada all occur in weakly-consolidated Paleogene and Neogene strata or Quaternary loose sediments with high porosity and high permeability (Majorowicz JA and Hannigan PK, 2000). They are mostly produced in the form of pore filling. However, marine hydrates mostly occur in Neogene or Quaternary loose sediments.

As cap rock, permafrost plays an important role in the formation of hydrates in permafrost in both the Plateau and Arctic permafrost regions. Permafrost serves to seal deep thermogenic gases from migrating upwards, thereby stopping hydrocarbon gases emission to the ground surface and then escape. Especially, in the North Slope of Alaska, USA and Mackenzie Delta, Canada, the permafrost can also isolate the underlying thermogenic gases from the overlying microbial gases. As a result, microbial gases are distributed in the upper

part, mixed gases in the middle, and thermogenic gases in the lower part. For marine hydrates, there is no distinctive cap rock, and hugely thick seawater and sediments play the role of blocking gases from migrating.

In terms of the formation era, hydrates in the Qilian Mountains possibly formed during 2.0–1.8 Ma BP, which is close to the formation era of hydrates in the North Slope of Alaska (around 1.8 Ma BP). Meanwhile, the NGH in the main body of the Plateau possibly formed later than 0.8 Ma BP.

The NGH in the Plateau formed as follows. As deep thermogenic gases migrate upwards along migration pathways such as faults, they were gradually enriched under the seal of permafrost and form NGH in the hydrate stability zones. This is basically the same in Messoyakha, Russia, but significantly different from the situation in the North Slope of Alaska, USA and Mackenzie Delta, Canada. The North Slope of Alaska and Mackenzie Delta are located in coastal areas and fall into the same hydrate-oil system as the Beaufort Sea (Majorowicz JA and Hannigan PK, 2000). Therefore, the formation mechanism and process of the hydrates in these two areas have the characteristics of both hydrates in permafrost and marine hydrates, which may be converted into each other as the permafrost degrades and the sea level changes.

Most of thermogenic gas hydrates are closely associated with the underlying oil and gas fields, especially in Arctic permafrost regions. Messoyakha, Russia, the North Slope of Alaska, USA, and Mackenzie Delta, Canada, are important oil & gas distribution areas (Collett TS et al., 2011; Dallimore SR and Collett TS, 1999). Though the Qiangtang Basin and South Qilian Basin are important target oil and gas exploration areas in China, no substantial breakthrough has ever been made so far, which may be a major factor restricting the prospecting discovery of NGH in the Plateau.

To sum up, the NGH in the Plateau are similar to those in Messoyakha, Russia, but they are considerably different from those in the North Slope of Alaska, USA and Mackenzie Delta, Canada and are even more different from marine hydrates.

5.2. NGH in permafrost regions and global climate change

NGH are important carbon depots in the Earth. About $2.1 \times 10^{16} \text{ m}^3$ of methane occurs in the form of hydrates worldwide, and the formation or dissociation of hydrates has a great impact on the environment. Therefore, NGH are a hot spot for the research on global climate change, and large numbers of studies had been made previously (Kvenvolden KA, 1993; Dickens GR et al., 1997; Kennett JP et al., 2000). The hydrates in permafrost are more sensitive to the environment. For example, hydrates in the Arctic have decomposed on a large scale over the recent 100 years of global warming, and the absolute methane quantity released accounts for about 39% of the total methane in the globe (Kretschmer K et al., 2015). This indicates that hydrates in permafrost are of great importance for the research of global climate change.

NGH provide both positive and negative feedbacks to

global climate change. For hydrates in permafrost, during the interglacial period when the globe warms and glaciers and ice sheets melt, the NGH in permafrost decompose due to the increase in temperature and decrease in pressure. As a result, methane is released and the greenhouse effect is generated. Therefore, they provide positive feedback to global warming, and vice versa. For marine hydrates, global warming will directly lead to an increase in the temperature of sea water and promote hydrates to decompose. However, due to the rise of the sea level, the submarine hydrostatic pressure will rise, which will improve the stability of NGH. Therefore, they produce both positive and negative feedback.

Under the background of global warming, the high-latitude regions in the Northern Hemisphere experienced a more significant warming process than other regions, resulting in permafrost degradation in Siberia, the Arctic Circle, Alaska, north Canada, northern Europe, and even the whole Northern Hemisphere. Most especially, the permafrost in the Arctic Circle is the most sensitive to temperature change. The warming process promotes the dissociation of NGH occurring beneath or within the permafrost. So far, many papers have reported the phenomenon of methane gas being released from NGH dissociation in the Arctic, North Atlantic Ocean, and North Pacific Ocean (Mestdagh T et al., 2017). The permafrost thickness and NGH in the North Slope of Alaska, USA and the Mackenzie Delta, Canada have constantly changed with glacial and interglacial cycles. In addition, the tectonic uplift and glacial advance and retreat during the Late Pliocene-Pleistocene in the southwestern Barents Sea shelf may also serve as a reason for NGH dissociation and natural gas seepage.

The permafrost and NGH in the Plateau are also very sensitive to global climate change. Under the background of global warming, the rate of increase in the temperature of the Plateau was twice as high as the global average rate and the permafrost degradation is more obvious over the past 50 years. All these will inevitably lead to NGH dissociation. According to preliminary research, if the temperature in the Plateau rises by 4.0°C at the end of this century, about 59.68% of NGH will decompose and release about 5.30×10^{12} m³ of methane, a large amount of which will be released into the atmosphere. This will inevitably further accelerate global warming, especially in the Plateau and its adjacent areas.

6. Conclusions

(i) The NGH in the Plateau have complex gas components and are dominated by deep thermogenic gas. They occur in the Permian–Jurassic strata and are subject to thin permafrost. Furthermore, they are distinctly different from the NGH in the arctic permafrost and in marine.

(ii) The formation of the NGH in the Plateau is obviously controlled by the uplift and permafrost evolution of the Plateau. The permafrost and NGH in the Qilian Mountains and the main body of the Qinghai-Tibet Plateau possible formed during 2.0–1.28 Ma BP and about 0.8 Ma BP,

respectively.

(iii) The permafrost and NGH in the Plateau are extreme sensitive to environmental changes. Under the background of global warming, continuous degradation of the permafrost will lead to NGH dissociation and methane release, thus further aggravating the warming of the Plateau and its adjacent areas.

CRedit authorship contribution statement

You-hai Zhu and Shou-ji Pang conceived of the presented idea. You-hai Zhu wrote the manuscript, and Shou-ji Pang and Rui Xiao designed the figures. Shuai Zhang and Zhen-quan Lu carried out the project. All authors discussed the results and contributed to the final manuscript.

Declaration of competing interest

The authors declare no conflicts of interest.

Acknowledgment

This study was funded by the project initiated by the China Geological Survey entitled *Comprehensive Survey of Terrestrial NGH Resources* (DD20190102). The authors would like to extend their sincere gratitude to the NGH field observation station in the Muli for the massive observation data. Thanks also go to Associate Researcher Guan-li Jiang from the Northwest Institute of Eco-Environment and Resources, CAS and Associate Researcher Ping-kang Wang from the China Geological Survey for their strong assistance in the preparation and review of this manuscript.

References

- An ZS, Wang SM, Wu XH, Chen MY, Sun DH, Liu XM, Wang FB, Li L, Sun YB, Zhou WJ, Zhou J, Liu XD, Lu HY, Zhang YX, Dong GR, Qiang XK. 1998. Eolian evidence from the Chinese Loess Plateau: The onset of the Late Cenozoic Great Glaciation in the Northern Hemisphere and Qinghai-Xizang Plateau uplift forcing. *Science in China (Series D)*, 42(3), 258–271. doi: [10.1360/zd1998-28-6-481](https://doi.org/10.1360/zd1998-28-6-481).
- Chen DF, Wang MC, Xia B. 2005. Formation condition and distribution prediction of gas hydrate in Qinghai-Tibet Plateau permafrost. *Chinese Journal of Geophysics*, 48(1), 165–172 (in Chinese with English abstract). doi: [10.1002/cjg2.638](https://doi.org/10.1002/cjg2.638).
- Cheng GD, Zhao L, Li R, Wu XD, Sheng Y, Hu GJ, Zou DF, Jin HJ, Li X, Wu QB. 2019. Characteristic, changes and impacts of permafrost on Qinghai-Tibet Plateau. *Chinese Science Bulletin*, 64(27), 2783–2795. doi: [CNKI:SUN:KXTB.0.2019-27-005](https://doi.org/CNKI:SUN:KXTB.0.2019-27-005).
- Collett TS, Kvenvolden KA, Magoon LB. 1990. Characterization of hydrocarbon gas within the stratigraphic interval of gas-hydrate stability on the North Slope of Alaska, U.S.A. *Applied Geochemistry*, 5(3), 279–287. doi: [10.1016/0883-2927\(90\)90003-N](https://doi.org/10.1016/0883-2927(90)90003-N).
- Collett TS, Lee MW, Agena WF, Miller JJ, Lewis KA, Zyrianova MV, Boswell R, Inks TL. 2011. Permafrost-associated natural gas hydrate occurrences on the Alaska North Slope. *Marine and Petroleum Geology*, 28(2), 279–294. doi: [10.1016/j.marpetgeo.2009.12.001](https://doi.org/10.1016/j.marpetgeo.2009.12.001).
- Dai JX, Ni YY, Huang SP, Peng WL, Han WX, Gong DY, Wei W. 2017. Genetic types of gas hydrates in China. *Petroleum Exploration and Development*, 44(6), 837–848 (in Chinese with English abstract).

- doi: [10.11698/PED.2017.06.01](https://doi.org/10.11698/PED.2017.06.01).
- Dai S, Lee C, Santamarina JC. 2011. Formation history and physical properties of sediments from the Mount Elbert Gas Hydrate Stratigraphic Test Well, Alaska North Slope. *Marine and Petroleum Geology*, 28(2), 427–438. doi: [10.1016/j.marpetgeo.2010.03.005](https://doi.org/10.1016/j.marpetgeo.2010.03.005).
- Dai S, Bao GY, Qi GM, Ma ZL, Bai WR, Yu D, Feng XL, Yang YH, Shi SB. 2019. Impacts of extreme climatic events under the context of climate warming on hydrology and water resources in the Qinghai Qilian Mountains. *Journal of Glaciology and Geocryology*, 41(5), 1053–1066 (in Chinese with English abstract). doi: [10.7522/j.issn.1000-0240.2019.0901](https://doi.org/10.7522/j.issn.1000-0240.2019.0901).
- Dallimore SR, Collett TS. 1999. Regional gas hydrate occurrences, permafrost conditions, and Cenozoic geology, Mackenzie Delta area//Dallimore SR, Uchida T, Collett TS. Scientific Results from JAPEx/JNOC/GSC Mallik 2L-38 Gas hydrate research well, Mackenzie Delta, Northwest Territories, Canada. *Bulletin of the Geological Survey of Canada*, 544, 31–43.
- Dickens GR, Castillo MM, Walker JC. 1997. A blast of gas in the latest Paleocene: Simulating first-order effect of massive dissociation of oceanic methane hydrate. *Geology*, 25, 259–262. doi: [10.1130/0091-7613\(1997\)025<0259:ABOGIT>2.3.CO;2](https://doi.org/10.1130/0091-7613(1997)025<0259:ABOGIT>2.3.CO;2).
- Ge XH, Liu JL, Ren SM, Yuan SH. 2014. Tectonic uplift of the Tibetan Plateau: Impacts on the formation of landforms, climate changes and ancient human migration in China. *Geology in China*, 41(3), 698–714 (in Chinese with English abstract).
- Gong JM, Zhang J, Chen XH, Liao J, Li XY, He XL, Jiang YB. 2014. Gas hydrate accumulation conditions between Qilian Mountain and Wuli permafrost region in Qinghai-Tibetan Plateau. *Journal of Oil and Gas Technology*, 36(2), 1–5 (in Chinese with English abstract). doi: [10.3969/j.issn.1000-9752.2014.02.001](https://doi.org/10.3969/j.issn.1000-9752.2014.02.001).
- Jiao SH, Wang LY, Liu GN. 2016. Prediction of Tibetan Plateau permafrost distribution in global warming. *Acta Scientiarum Naturalium Universitatis Pekinensis*, 52(2), 249–256 (in Chinese with English abstract). doi: [10.13209/j.0479-8023.2015.112](https://doi.org/10.13209/j.0479-8023.2015.112).
- Jiao SH, Wang LY, Sun CQ, Yi ZL, Cui ZJ, Liu GN. 2015. Discussion about the variation of permafrost boundary in last glacial maximum and Holocene megathermal, Tibetan plateau. *Quaternary Sciences*, 35(1), 1–11 (in Chinese with English abstract). doi: [10.11928/j.issn.1001-7410.2015.01.01](https://doi.org/10.11928/j.issn.1001-7410.2015.01.01).
- Jin HJ, Jin XY, He RX, Luo DL, Chang XL, Wang SL, Smarchenko S, Yang SZ, Yi ZL, Li SJ, Aharris S. 2019. Evolution of permafrost in China during the last 20 ka. *Science China Earth Sciences*, 62, 1197–1212. doi: [10.1360/N072018-00035](https://doi.org/10.1360/N072018-00035).
- Kennett JP, Cannariato KG, Hendy IL, Behl RJ. 2000. Carbon isotopic evidence for methane hydrate instability during Quaternary interstadials. *Science*, 288, 128–133. doi: [10.1126/science.288.5463.128](https://doi.org/10.1126/science.288.5463.128).
- Kneafsey TJ, Lu H, Winters W, Boswell R, Hunter R, Collett TS. 2011. Examination of core samples from the Mount Elbert gas hydrate stratigraphic test well, Alaska North Slope: Effects of retrieval and preservation. *Marine and Petroleum Geology*, 28(2), 381–393. doi: [10.1016/j.marpetgeo.2009.10.009](https://doi.org/10.1016/j.marpetgeo.2009.10.009).
- Kretschmer K, Biastoch A, Rüpke L, Burwicz E. 2015. Modeling the fate of methane hydrates under global warming. *Global Biogeochemical Cycles*, 29(5), 610–625. doi: [10.1002/2014GB005011](https://doi.org/10.1002/2014GB005011).
- Ku XB, Wu QB, Jiang GL. 2007. Potential distribution of natural gas hydrate in the permafrost regions of Qinghai-Tibet Plateau. *Natural Gas Industry*, 18(4), 588–592 (in Chinese with English abstract). doi: [10.3969/j.issn.1672-1926.2007.04.022](https://doi.org/10.3969/j.issn.1672-1926.2007.04.022).
- Kvenvolden KA. 1988. Methane hydrate—a major reservoir of carbon in the shallow geosphere? *Chemical Geology*, 71, 41–51. doi: [10.1016/0009-2541\(88\)90104-0](https://doi.org/10.1016/0009-2541(88)90104-0).
- Kvenvolden KA. 1993. Gas hydrates-geological perspective and global change. *Chemical Geology*, 31(2), 173–187. doi: [10.1029/93RG00268](https://doi.org/10.1029/93RG00268).
- Li B, Sun YH, Guo W, Shan XL, Wang PK, Pang SJ, Jia R, Zhang GB. 2017. The mechanism and verification analysis of permafrost-associated gas hydrate formation in the Qilian Mountain, Northwest China. *Marine and Petroleum Geology*, 86, 787–197. doi: [10.1016/j.marpetgeo.2017.05.036](https://doi.org/10.1016/j.marpetgeo.2017.05.036).
- Li JJ. 2013. Uplift of the Qinghai-Tibet Plateau and environmental evolution of late Cenozoic. *Journal of Lanzhou University (Natural Science)*, 49(2), 154–159 (in Chinese with English abstract). doi: [10.3969/j.issn.0455-2059.2013.02.002](https://doi.org/10.3969/j.issn.0455-2059.2013.02.002).
- Li QL, Wang XW. 2003. Quaternary environmental changes in western Qilian Mountains, Gansu. *Sedimentary Geology and Tethyan Geology*, 23(2), 43–47 (in Chinese with English abstract). doi: [10.3969/j.issn.1009-3850.2003.02.008](https://doi.org/10.3969/j.issn.1009-3850.2003.02.008).
- Li SX, Cheng GD. 1996. The analysis and approximate calculation of permafrost evolution. *Journal of Glaciology and Geocryology*, 18(Special issue), 197–205 (in Chinese with English abstract). doi: [CNKI:SUN:BCDT.0.1996-S1-023](https://doi.org/CNKI:SUN:BCDT.0.1996-S1-023).
- Li X, Cheng GD. 1999. Response model of global climate change in the high-elevation permafrost. *Science China Earth Science*, 29(2), 185–192. doi: [10.3321/j.issn:1006-9267.1999.02.011](https://doi.org/10.3321/j.issn:1006-9267.1999.02.011).
- Liu GY, Zhao L, Xie CW, Pang QQ, Du RJ, Qiao YP. 2016. Variation characteristics and impact factors of the depth of zero annual amplitude of ground temperature in permafrost regions on the Tibetan Plateau. *Journal of Glaciology and Geocryology*, 38(5), 1189–1200 (in Chinese with English abstract). doi: [10.7522/j.issn.1000-0240.2016.0139](https://doi.org/10.7522/j.issn.1000-0240.2016.0139).
- Liu H, Zhu YH, Pang SJ, Zhang YQ, Liang J, Zhang JZ. 2019. Important evidence for gas hydrate occurrence in Wuli, Qinghai Province. *Geology in China*, 46(5), 1243–1244 (in Chinese with English abstract). doi: [CNKI:SUN:DIZL.0.2019-05-027](https://doi.org/CNKI:SUN:DIZL.0.2019-05-027).
- Lorenson TD, Collett TS, Hunter RB. 2011. Gas geochemistry of the Mount Elbert gas hydrate stratigraphic test well, Alaska North Slope: implications for gas hydrate exploration in the arctic. *Marine and Petroleum Geology*, 2011, 343–360. doi: [10.1016/j.marpetgeo.2010.02.007](https://doi.org/10.1016/j.marpetgeo.2010.02.007).
- Lorenson TD, Whiticar MJ, Waseda A. 1999. Gas composition and isotopic geochemistry of cuttings, core, and gas hydrate from the JAPEx/JNOC/GSC Mallik 2L-38 gas hydrate research well//Dallimore SR, Uchida T, Collett TS. Scientific Results from JAPEx/JNOC/GSC Mallik 2L-38 Gas Hydrate Research Well, Mackenzie Delta, Northwest Territories, Canada. *Bulletin of the Geological Survey of Canada*, 544, 143–163.
- Lu J, Chen MH. 2006. Global climate events since Cenozoic. *Journal of Tropical Oceanography*, 25(6), 72–79 (in Chinese with English abstract). doi: [10.3969/j.issn.1009-5470.2006.06.013](https://doi.org/10.3969/j.issn.1009-5470.2006.06.013).
- Lu ZQ, Zhai GY, Zhu YH, Liu H, Wang T, Fang H, Sun ZJ, Tang SQ, Zhang YQ. 2018. New discovery of the permafrost gas hydrate accumulation in Qilian Mountain, China. *China Geology*, 1, 306–307. doi: [10.31035/cg2018034](https://doi.org/10.31035/cg2018034).
- Lu ZQ, Tang SQ, Luo XL, Zhai GY, Fan DW, Liu H, Wang T, Zhu YH, Xiao R. 2020. A natural gas hydrate-oil-gas system in the Qilian Mountain permafrost area, northeast of Qinghai-Tibet Plateau. *China Geology*, 3, 511–523. doi: [10.31035/cg2020075](https://doi.org/10.31035/cg2020075).
- Lu ZQ, Zhu YH, Zhang YQ, Wen HJ, Li YH, Liu CL. 2011. Gas hydrate occurrences in the Qilian Mountain permafrost, Qinghai Province, China. *Cold Regions Science and Technology*, 66(2–3), 93–104. doi: [10.1016/j.coldregions.2011.01.008](https://doi.org/10.1016/j.coldregions.2011.01.008).
- Luo DL, Jin HJ, Lin L, He RX, Yang SZ, Chang XL. 2012. New progress on permafrost temperature and thickness in the source area of the Huanghe River. *Scientia Geographica Sinica*, 32(7), 898–904 (in Chinese with English abstract). <http://ir.casnw.net/handle/362004/8861>
- Majorowicz JA, Osadetz K. 2001. Basic geological and geophysical

- indications of gas hydrate distribution and volume in Canada. *American Association of Petroleum Geologists Bulletin*, 85, 1211–1230.
- Majorowicz JA, Hannigan PK. 2000. Natural gas hydrates in the offshore Beaufort-Mackenzie basin—study of a feasible energy source. *Natural Resources Research*, 9(3), 201–214. doi: [10.1023/A:1010179301059](https://doi.org/10.1023/A:1010179301059).
- Makogon YF, Holditch SA, Makogon TY. 2007. Natural gas-hydrates—a potential energy source for the 21st Century. *Journal of Petroleum Science and Engineering*, 56(1–3), 14–31. doi: [10.1016/j.petrol.2005.10.009](https://doi.org/10.1016/j.petrol.2005.10.009).
- Mestdagha T, Poortb J, De Batista M. 2017. The sensitivity of gas hydrate reservoirs to climate change: Perspectives from a new combined model for permafrost-related and marine settings. *Earth-Science Reviews*, 169, 104–131. doi: [10.1016/j.earscirev.2017.04.013](https://doi.org/10.1016/j.earscirev.2017.04.013).
- Milkov AV. 2004. Global estimates of hydrate-bound gas in marine sediments, how much is really out there? *Earth-Science Reviews*, 66(3–4), 183–197. doi: [10.1016/j.earscirev.2003.11.002](https://doi.org/10.1016/j.earscirev.2003.11.002).
- Pan BT, Li JJ, Zhu JJ, Cao JX. 1995. Qinghai-Tibetan Plateau: A driver and amplifier of the global climatic changes – II. Uplift Progresses of the Qinghai-Xizang(Tibetan) Plateau. *Journal of Lanzhou University (Natural Science)*, 31(4), 160–167 (in Chinese with English abstract). doi: [CNKI:SUN:LDZK.0.1995-04-029](https://doi.org/CNKI:SUN:LDZK.0.1995-04-029).
- Qi BS, Hu DG, Zhao XT, Zhang XJ, Zhang YL, Yang XX, Zhao Z, Gao XM. 2014. Fossil sand wedges in the northern shore of Qinghai Lake: Discovery and paleoclimatic implications. *Journal of Glaciology and Geocryology*, 36(6), 1412–1419 (in Chinese with English abstract). doi: [10.7522/j.issn.1000-0240.2014.0168](https://doi.org/10.7522/j.issn.1000-0240.2014.0168).
- Qiao YC, Zhao GP, Shi YL, Liu TQ. 2010. Numerical simulation of influence of the Qinghai-Tibet Plateau rising rates on formation of Permafrost. *Acta Geologica Sinica*, 84(6), 901–908 (in Chinese with English abstract). doi: [CNKI:SUN:DZXE.0.2010-06-016](https://doi.org/CNKI:SUN:DZXE.0.2010-06-016).
- Ruppel C. 2015. Permafrost-associated gas hydrate: Is it really approximately 1% of the global system? *Journal of Chemical and Engineering Data*, 60(2), 429–436. doi: [10.1021/je500770m](https://doi.org/10.1021/je500770m).
- Shi YF, Li JJ, Li BY, Yao TD, Wang SM, Li SJ, Cui ZJ, Wang FB, Pan BT, Fang XM, Zhang QS. 1999. Uplift of the Qinghai-Xizang (Tibetan) Plateau and East Asia environmental changes during late Cenozoic. *Acta Geographica Sinica*, 54(1), 10–21. doi: [10.3321/j.issn:0375-5444.1999.01.002](https://doi.org/10.3321/j.issn:0375-5444.1999.01.002).
- Shi YF, Zheng BX, Yao TD. 1997. Glaciers and environments during the Last Glacial Maximum (LGM) on the Tibetan Plateau. *Journal of Glaciology and Geocryology*, 19, 97–113 (in Chinese with English abstract). doi: [CNKI:SUN:BCDT.0.1997-02-000](https://doi.org/CNKI:SUN:BCDT.0.1997-02-000).
- Wang PK, Zhu YH, Lu ZQ, Bai MG, Huang X, Pang SJ, Zhang S, Liu H, Xiao R. 2019. Research progress of gas hydrates in the Qilian Mountain permafrost, Qinghai, Northwest China: Review. *Scientia Sinica Physica, Mechanica & Astronomica*, 49(3), 034606 (in Chinese with English abstract). doi: [10.1360/SSPMA2018-00133](https://doi.org/10.1360/SSPMA2018-00133).
- Wang X, Pan L, Lau HC, Zhang M, Li LL, Zhou Q. 2018. Reservoir volume of gas hydrate stability zones in permafrost regions of China. *Applied Energy*, 225, 486–500. doi: [10.1016/j.apenergy.2018.04.125](https://doi.org/10.1016/j.apenergy.2018.04.125).
- Wu QB, Jiang GL, Zhang P, Deng YS, Yang YZ, Hou YD, Zhang BG. 2015. Evidence of natural gas hydrate in Kunlun Pass basin, Qinghai-Tibet Plateau, China. *Chinese Science Bulletin*, 60, 68–74 (in Chinese with English abstract). doi: [10.1360/n972014-00088](https://doi.org/10.1360/n972014-00088).
- Xiao HP, Wu QB, Lin CS, Wei W, Zhang JH, Peng Y, Zhang P, Zhang QZ. 2016. Preliminary discussion on the space-time coupling of natural gas hydrate accumulation elements: A case study from Kunlun Pass permafrost regions, Qinghai-Tibet Plateau. *Natural Gas Geoscience*, 27(10), 1913–1923 (in Chinese with English abstract). doi: [10.11764/j.issn.1672-1926.2016.10.1913](https://doi.org/10.11764/j.issn.1672-1926.2016.10.1913).
- Xu XZ, Cheng GD, Yu QH. 1999. Research prospect and suggestions of gas hydrates in permafrost regions on the Qinghai-Tibet Plateau. *Advances in Earth Science*, 14(2), 201–204 (in Chinese with English abstract). doi: [10.3321/j.issn:1001-8166.1999.02.018](https://doi.org/10.3321/j.issn:1001-8166.1999.02.018).
- Yao TD. 2019. A comprehensive study of water-ecosystem-human activities reveals unbalancing Asian Water Tower and accompanying potential risks. *Chinese Science Bulletin*, 64(27), 2761–2762 (in Chinese with English abstract). doi: [CNKI:SUN:XXTB.0.2019-27-001](https://doi.org/CNKI:SUN:XXTB.0.2019-27-001).
- Zhao XM, Song FY, Deng J, Rao Z, Wen ZG, Hu DG, Yi L, Liu C. 2018. New indications of gas hydrate in the northeastern China permafrost zone. *China Geology*, 1, 308–309. doi: [10.31035/cg2018033](https://doi.org/10.31035/cg2018033).
- Zhang JH, Wei W, Wei XH, Xiao HP, Peng Y, Zhang QQ, Wang P. 2016. Formation conditions of natural gas hydrates in Kunlun Mountain Pass Basin. *Unconventional Oil & Gas*, 3(3), 101–105 (in Chinese with English abstract). doi: [CNKI:SUN:FCYQ.0.2016-03-018](https://doi.org/CNKI:SUN:FCYQ.0.2016-03-018).
- Zhang WJ, Cheng WM, Li BL, Tong CM, Zhao M, Wang N. 2014. Simulation of the permafrost distribution on Qilian Mountains over past 40 years under the influence of climate change. *Geographical Research*, 33(7), 1275–1284 (in Chinese with English abstract). doi: [10.11821/dlyj201407008](https://doi.org/10.11821/dlyj201407008).
- Zhong DB, Ding L. 1996. Rising process of the Qinghai-Xizang (Tibet) Plateau and its mechanism. *Science in China (Series D)*, 39(4), 369–379. doi: [CNKI:SUN:JDXG.0.1996-04-003](https://doi.org/CNKI:SUN:JDXG.0.1996-04-003).
- Zheng D, Lin ZY, Zhang XQ. 2002. Progress in studies of Tibetan plateau and global environmental change. *Earth Science Frontiers*, 9(1), 95–102 (in Chinese with English abstract). doi: [10.3321/j.issn:1005-2321.2002.01.012](https://doi.org/10.3321/j.issn:1005-2321.2002.01.012).
- Zhou Q, Li WL, Chen WT, Wang YJ. 2011. Spatial coupling relationships about formation of gas hydrate in Tibetan Plateau. *Journal of Glaciology and Geocryology*, 33(5), 1139–1145 (in Chinese with English abstract). doi: [CNKI:SUN:BCDT.0.2011-05-025](https://doi.org/CNKI:SUN:BCDT.0.2011-05-025).
- Zhou SZ, Li JJ. 2003. Recent progress in the study on Quaternary glaciation in China. *Journal of Glaciology and Geocryology*, 25(6), 660–666 (in Chinese with English abstract). doi: [10.3969/j.issn.1000-0240.2003.06.011](https://doi.org/10.3969/j.issn.1000-0240.2003.06.011).
- Zhou YW, Guo DX, Qiu GQ, Cheng GD, Li SD. 2000. *Geocryology in China*. Beijing, Science Press, 1–245 (in Chinese). <https://doi.org/10.2307/1552227>
- Zhu YH, Zhang YQ, Wen HJ, Jia ZY, Li YH, Li QH, Liu CL, Wang PK, Guo XW. 2010. Gas hydrates in the Qilian Mountain permafrost, Qinghai, Northwest China. *Acta Geologica Sinica (English Edition)*, 84(1), 1–10. doi: [10.1111/j.1755-6724.2010.00164.x](https://doi.org/10.1111/j.1755-6724.2010.00164.x).
- Zhu YH, Zhao SM, Lu ZQ. 2011. Resource potential and reservoir distribution of natural gas hydrate in permafrost areas of China. *Natural Gas Industry*, 31(1), 13–19 (in Chinese with English abstract). doi: [10.3787/j.issn.1000-0976.2011.01.003](https://doi.org/10.3787/j.issn.1000-0976.2011.01.003).